2013 American Control Conference (ACC)
Washington, DC, USA, June 17-19, 2013

Introduction to Wide-Area Control of Power Systems

Aranya Chakrabortty[1] and Pramod P. Khargonekar[2]
[1]North Carolina State University, [2] University of Florida
Emails: [1]achakra2@ncsu.edu, [2]ppk@ufl.edu

Abstract— **A key element in the development of smart power transmission systems over the past decade is the tremendous advancement of the Wide-Area Measurement System (WAMS) technology, also commonly referred to as the *Synchrophasor* technology. Sophisticated digital recording devices called Phasor Measurement Units or PMUs are currently being installed at different points in the North American grid, especially under the smart grid initiatives of the US Department of Energy, to record and communicate GPS-synchronized, high sampling rate (6-60 samples/sec), dynamic power system data. Significant research efforts have been made on techniques to use WAMS for monitoring and situational awareness of large power networks dispersed across wide geographical areas. In contrast, use of WAMS for automatic feedback control has received less attention from the research community. The objective of this paper is to bridge this gap by formulating wide-area control problems for oscillation damping, voltage control, wide-area protection, and disturbance localization. We present the main research challenges that need to be overcome to realize the benefits of wide area control in power systems. Our discussion begins with a review of the fundamental physical models of different characteristic components of a large transmission-level power grid such as synchronous generators, transmission lines, and loads, followed by a description of how these subsystem-level models can be integrated to form the overall system model. We pose ten distinct control-theoretic problems. The first two problems are on using PMU measurements from selected nodes in the system to identify such system models in different resolutions in real-time, and the remaining on how the identified models can be used for designing output-feedback based damping controllers, for understanding voltage fluctuations at different nodes of the network graph, and for detecting malicious inputs entering the system dynamics via faults or extraneous attacks. We also propose two new control paradigms, namely a scheduling approach for appropriate controller selection based on online estimation of oscillation modes, and distributed phasor-based control using model estimation. We illustrate our ideas via representative examples, many of which are inspired by well-known power transfer paths in the US west coast grid, also referred to as the Western Electricity Coordinating Council (WECC).**

Index Terms— **Synchronized Phasor Measurements, Wide-Area Control, Oscillation Damping, Real-time Identification, Model Reduction, Distributed Control, FACTS, IEEE C37.118, Network Delays, Excitation Control, NASPInet.**

I. Introduction

In the coming decades, electric power grids are envisioned to become green and smart. Motivated by catastrophic failures such as the 2003 blackout in the Northeastern USA and Hurricane Katrina in 2005, the Energy Act of 2007, concerns over carbon emissions from fossil fuel based power generation, and the critical need for a cost effective electric energy system, the concept of smart grid has become almost ubiquitous across the world. It is both a socio-economic-regulatory concept and also a new engineering/technology vision. One key component of smart grid development over the past decade is the deployment of measurement and instrumentation systems, especially in the form of the Wide-Area Measurement System (WAMS) technology, also commonly referred to as the Synchrophasor technology [1]. Sophisticated digital recording devices called Phasor Measurement Units or PMUs are currently being installed at different points in the North American grid, especially under the smart grid initiatives of the US Department of Energy. Analogous deployment of PMUs is also underway in different regions of the world. These devices record and communicate GPS-synchronized, high sampling rate (6-60 samples/sec), dynamic power system data. Research platforms such as the North American Synchrophasor Initiative (NASPI) [2] and the Western Interconnection Synchrophasor Project (WISP) [3] have been formed to investigate how Synchrophasors can be exploited to track or *keep an eye* on the dynamic health of geographically dispersed large power networks [4].

Concerted efforts are currently being made to develop nationwide 'early warning' mechanisms using PMU measurements that will enable power system operators to take timely actions against blackouts and other widespread contingencies. Excellent visualization tools, for example, in the form of Real Time Dynamics Monitoring System (RTDMS) developed by the Electric Power Group [5] and US-Wide Frequency Monitoring Network (FNET) developed at University of Tennessee [6] are currently being deployed across the US grid. This development has been complemented by an equally remarkable progress in data analysis methods and software platforms, some leading examples being the Dynamic System Identification (DSI) software developed by the Pacific Northwest National Laboratory [7], [8], wide-area oscillation detection by frequency-domain optimization methods [9], Hilbert-Huang transforms [10], and phasor-based state estimation [11], [12], [13].

However, most of the research done so far in this direction only addresses *monitoring* and *observation*. Relatively modest efforts have been made to explore how Synchrophasors can also be used for *automatic feedback control* [14], [15], [16], [17]. More than 132 PMUs are currently operating in the US West Coast power system (WECC), and nearly 80 PMUs in the Eastern Interconnect (EI), (and much larger numbers of PMUs expected in the coming years), and they produce over 2 billion data samples per day. As such, control by human operators is obviously not sustainable.

An autonomous, highly distributed, bandwidth-efficient, real-time control system will be needed to fully utilize the value of wide spread Synchrophasor deployment.

Our objective in this paper is to address the need for formulations and presentations of wide area control problems that are accessible to the control systems community. We focus on four major power systems control applications:

1) Power oscillation damping
2) Voltage stability
3) Disturbance localization
4) New control paradigms such as distributed and adaptive control.

We present the main research challenges that need to be overcome to realize the benefits of wide area control. Our discussion begins with a review of the fundamental physical models of different characteristic components of a large transmission-level power grid such as synchronous generators, transmission lines, and loads, followed by a description of how these subsystem-level models can be integrated to form the overall system model. We pose ten distinct systems/control problems. The first two problems are focused on using PMU measurements from selected nodes in the system to identify such system models in real-time, and the remaining on how the identified models can be used for designing output-feedback based damping controllers, for understanding voltage fluctuations at different nodes of the network graph, and for detecting malicious inputs entering the system dynamics via faults or extraneous attacks. We also propose two new control paradigms, namely a scheduling approach for appropriate controller selection based on online estimation of oscillation modes, and distributed phasor-based control using model estimation. We illustrate our ideas via representative examples many of which are inspired by well-known power transfer paths in the US west coast grid, also referred to as the Western Electricity Coordinating Council (WECC).

The remainder of the paper is organized as follows. Section II develops the model for the swing dynamics and excitation dynamics of a multi-machine power system network. Section III presents two problems on model identification using PMU measurements, Section IV formulates the wide-area damping control problem, and Section VI presents the problem of disturbance localization. Section VII presents two new control approaches for wide-area damping. Section VIII concludes the paper.

II. Power System Models

The primary idea behind wide-area control of power systems is to develop control designs, either in a centralized or in a distributed architecture, over *wide areas* across the grid, so that the closed-loop stability and performance of the grid can be assured from a higher level of system integration. The goal is to address a much larger-scale control problem than the current *local* control methods such as Automatic Generation Control, local PSS damping, fast valving, etc. Formulation of these wide-area control problems requires a thorough understanding of the global dynamic model of the system for the relevant application. This is particularly important for power oscillation damping where it is necessary to model the dynamic evolution of oscillations in the line flows at different frequencies and design controllers to achieve the desired damping. We, therefore, begin our discussion by reviewing the fundamental oscillation dynamics of a typical power system, and explain how the network structure as well as its model parameters can result in time-scale separation between fast and slow oscillations.

A. Synchronous Generator Models

Consider a power system network with n buses. Without loss of generality, classify the first n_1 buses to be *generator buses*, meaning that these buses are directly connected to a synchronous generator operating at a steady-state frequency of 60 Hz or 120π radian/second, and the remaining $(n-n_1)$ buses as *load buses* meaning that active and reactive power are extracted from these buses in the form of loads. Since this is an AC power system, the voltages and currents in the network will be complex numbers, each denoted by a magnitude and phase angle. The voltage at the i^{th} bus is denoted as $\tilde{V}_i = V_i \angle \theta_i$ where V_i is the magnitude (volts) and θ_i is the phase (radians). The internal voltage phasor of a synchronous generator connected to any generator bus is denoted as $\tilde{E}_i = E_i \angle \delta_i$, $i = 1, 2, ..., n_1$. Each synchronous generator may be modeled by a set of third-order differential algebraic equations [18]

$$\dot{\delta}_i = \omega_i - \omega_s \tag{1}$$

$$M_i \dot{\omega}_i = P_{mi} - D_i(\omega_i - \omega_s) - P_i^G \tag{2}$$

$$\tau_i \dot{E}_i = -\frac{x_{di}}{x'_{di}} E_i + \frac{x_{di} - x'_{di}}{x'_{di}} V_i \cos(\delta_i - \theta_i) + E_{Fi} \tag{3}$$

$$P_i^G = \frac{E_i V_i}{x'_d{}^i} \sin(\delta_i - \theta_i) + \left(\frac{x'_{di} - x_{qi}}{2 x_{qi} x'_{di}} \right) V_i^2 \sin(2(\delta_i - \theta_i)) \tag{4}$$

$$Q_i^G = \frac{E_i V_i}{x'_d{}^i} \cos(\delta_i - \theta_i) - \left(\frac{x'_{di} - x_{qi}}{2 x_{qi} x'_{di}} - \frac{x'_{di} - x_{qi}}{2 x_{qi} x'_{di}} \cos(2(\delta_i - \theta_i)) \right) V_i^2 \tag{5}$$

where, the states δ_i, ω_i and E_i are, respectively, the generator phase angle (radians), rotor velocity (rad/sec), and the quadrature-axis internal emf; ω_s is the synchronous frequency or 120π radian/sec; P_i^G and Q_i^G are, respectively, the active and reactive power produced by the i^{th} generator (Mega Watts and Mega VAr), M_i is the generator inertia (seconds), D_i is the generator damping, P_{mi} is the mechanical power input from the i^{th} turbine (Mega Watts); τ_i is the excitation time constant (seconds); x_{di}, x'_{di}, and x_{qi} are the direct-axis salient reactance, direct-axis transient reactance, and quadrature-axis salient reactance (all in ohms), respectively. The variables V_i and θ_i are *algebraic* variables, meaning that they are not direct state variables but only algebraic functions of the state variables that follow from (4)-(5). The control variable is the field voltage E_{Fi}, which can be split in two separate terms

$$E_{Fi} = \bar{E}_{Fi} + E_i \tag{6}$$

where, the first term is a constant that fixes the equilibrium value, and the second is a designable control input that

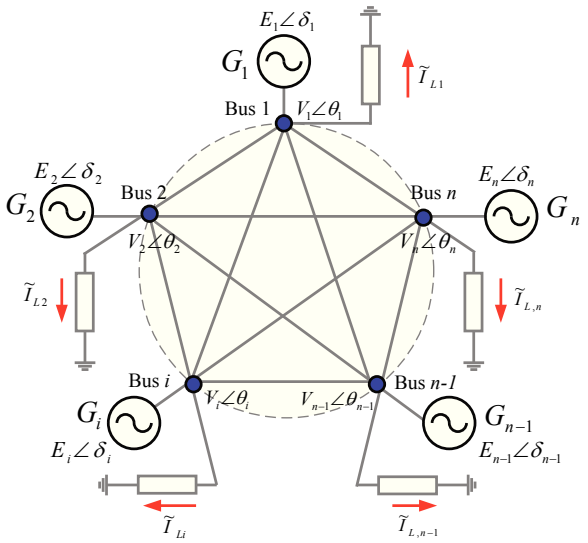

Fig. 1. n-bus power system network with full connectivity

can be applied via state feedback or output feedback. This input is commonly referred to as *excitation control*. Detailed description of the various parameters of the model (1)-(5) can be found in [19]. Illustrative examples of excitation control designs can be found in [18], [20].

B. Load Models

The active and reactive power drawn by the j^{th} load, where $j = n_1 + 1, n_1 + 2, ..., n$, can be modeled as [20]

$$P_j^L = a_j V_j^2 + b_j V_j + c_j, \;\; Q_j^L = e_j V_j^2 + f_j V_j + g_j \quad (7)$$

where, $(a_j,\, b_j,\, c_j)$ and $(e_j,\, f_j,\, g_j)$ are load-specific constant coefficients of appropriate dimension, and the three terms in each equation explicitly represent the contribution of each type of load, namely, constant impedance, constant current and constant power load, respectively.

C. Transmission Line Models

A transmission line connecting the i^{th} bus (sending end) to the j^{th} bus (receiving end) is modeled by a standard lumped parameter π-model, where the active and reactive powers transferred across the line are given as [20], [21]

$$\begin{aligned} P_{ij} &= G_{ij}V_i^2 + B_{ij}V_iV_j\sin(\theta_i-\theta_j) - G_{ij}V_iV_j\cos(\theta_i-\theta_j) \\ Q_{ij} &= (B_{ij}-B_{ij}^c)V_i^2 - B_{ij}V_iV_j\cos(\theta_i-\theta_j) - G_{ij}V_iV_j\sin(\theta_i-\theta_j). \end{aligned}$$

Here, $G_{ij} = G_{ji}$ is the line conductance, $B_{ij} = B_{ji}$ is the line series succeptance, and $B_{ij}^c = B_{ji}^c$ is the line shunt succeptance connecting bus i to bus j, all in mhos. If bus i and bus j are not connected then all these three quantities are zero.

D. Network Dynamic Models

Equations (1)-(2) follow from Newton's second law of motion applied to the internal states of the i^{th} generator. The algebraic variables at any bus, however, follow Kirchoff's law manifesting in the form of active and reactive power balance

$$0 = \sum_{k\in\mathcal{N}_i} P_{ik} - P_i^G, \;\; 0 = \sum_{k\in\mathcal{N}_i} Q_{ik} - Q_i^G, \quad (8)$$

$$0 = \sum_{k\in\mathcal{N}_j} P_{jk} + P_j^L, \;\; 0 = \sum_{k\in\mathcal{N}_j} Q_{jk} + Q_j^L, \quad (9)$$

where, $i = 1, ..., n_1$, $j = n_1 + 1, n_1 + 2, ..., n$, $\mathcal{N}_i$ denotes the set of bus numbers that are connected to bus i, i.e., the neighbor set of bus i. The dynamical model for the entire system can be constructed by relating the generator models, load models and transmission line models over any given interconnection of the n buses making use of the power balance equations (8)-(9). To achieve this in the most generic way, consider the network to be of the form shown in Figure 1, where each of the n buses is assumed to be connected to a generator as well as to a load. The transmission lines are assumed to have both resistance and reactance, and are modeled by π-models. For simplicity of notations we also assume that every bus is connected to every other bus. If in reality, any two buses are not connected then the corresponding line impedance must be substituted by infinity (or, equivalently the line admittance by zero). If any bus i does not have any load extracted from it then the load powers P_i^L and Q_i^L must simply be substituted by zero. If any bus i does not have a generator connected to it then M_i may be substituted by zero, and x_{di}, x'_{di} and x_{qi} must all be substituted by infinity. Next, consider a small perturbation over an existing equilibrium $(\delta_{i0},\, \omega_s,\, E_{i0},\, V_{i0},\, \theta_{i0})$, $i = 1, ..., n$. From (4) the change in the active power flowing out of the i^{th} generator can be written as

$$\Delta P_i^G = C_{1i}\Delta E_i + C_{2i}\Delta V_i + C_{3i}\Delta\delta_i + C_{4i}\Delta\theta_i \quad (10)$$

where, the expressions for C_{ji} with $j = 1(1)4$ and Y_{2i} can be found in [22], and are skipped here for brevity. The algebraic variables can be related to the states using Kirchoff's current law (KCL) at every bus. After a few calculations it can be shown that the exact expression of the algebraic variables in terms of the states is given as

$$\begin{bmatrix} \Delta V \\ \Delta\theta \end{bmatrix} = \underbrace{\Pi^{-1}\Psi}_{:=F} \begin{bmatrix} \Delta\delta \\ \Delta E \end{bmatrix} + \underbrace{\Pi^{-1}\begin{bmatrix} \Lambda_1 \\ \Lambda_2 \end{bmatrix}}_{:=G} \quad (11)$$

where,

$$\Pi = \begin{bmatrix} \mathrm{diag}(\cos(\theta_{i0})) & -\mathrm{diag}(V_{i0}\sin(\theta_{i0})) \\ \mathrm{diag}(\sin(\theta_{i0})) & -\mathrm{diag}(V_{i0}\cos(\theta_{i0})) \end{bmatrix} \quad (12)$$

$$\Psi = \left[\begin{array}{c|c} \Psi_1 & \Psi_2 \\ \hline \Psi_3 & \Psi_4 \end{array}\right] \quad (13)$$

$$\Psi_1 := -Y_{R1}\mathrm{diag}(E_i\sin(\delta_{i0})) - Y_{I1}\mathrm{diag}(E_i\cos(\delta_{i0})) \quad (14)$$

$$\Psi_2 := Y_{R1}\mathrm{diag}(\cos(\delta_{i0})) - Y_{I1}\mathrm{diag}(\cos(\delta_{i0})) \quad (15)$$

$$\Psi_3 := Y_{R1}\mathrm{diag}(E_i\cos(\delta_{i0})) - Y_{I1}\mathrm{diag}(E_i\sin(\delta_{i0})) \quad (16)$$

$$\Psi_4 := Y_{R1}\mathrm{diag}(\sin(\delta_{i0})) + Y_{I1}\mathrm{diag}(\cos(\delta_{i0})). \quad (17)$$

Next partition F into $(n \times n)$ blocks, and G into $(n \times 1)$ blocks as

$$F = \begin{bmatrix} F_1 & F_2 \\ F_3 & F_4 \end{bmatrix}, \quad G = \begin{bmatrix} G_1 \\ G_2 \end{bmatrix} \tag{18}$$

so that

$$\Delta V = F_1\Delta\delta + F_2\Delta E + G_1 \tag{19}$$
$$\Delta\theta = F_3\Delta\delta + F_4\Delta E + G_2. \tag{20}$$

Equations (19)-(20) give the exact relationship of the algebraic variables and the state variables for the entire network. Next, linearize (2) about the given equilibrium to get

$$M_i\Delta\dot{\omega}_i = \Delta P_{mi} - D_i\Delta\omega - (C_{1i}\Delta E_i + C_{2i}\Delta V_i + C_{3i}\Delta\delta_i + C_{4i}\Delta\theta_i).$$

Similarly, linearize (3) about the given equilibrium to obtain

$$\tau_i\Delta\dot{E}_i = a_i\Delta E_i + b_i\Delta V_i - e_i\Delta\delta_i + e_i\Delta\theta_i + \Delta E_i \tag{21}$$

where, ΔE_i denotes the designable excitation control input, and the constants $a_i := -x_{di}/x'_{di}$, $b_i := (x_{di}-x'_{di})\cos(\delta_{i0}-\theta_{i0})/x'_{di}$, $e_i := V_{i0}(x_{di}-x'_{di})\sin(\delta_{i0}-\theta_{i0})/x'_{di}$. From equations (19)-(21), the overall linearized $(3n)^{th}$-order dynamic model of the network can finally be expressed as

$$\begin{bmatrix} \Delta\dot{\delta} \\ M\Delta\dot{\omega} \\ T\Delta\dot{E} \end{bmatrix} = \underbrace{\begin{bmatrix} 0 & I & 0 \\ -L & -D & -P \\ K & 0 & J \end{bmatrix}}_{\mathcal{A}} \begin{bmatrix} \Delta\delta \\ \Delta\omega \\ \Delta E \end{bmatrix} + \underbrace{\begin{bmatrix} 0 \\ [\gamma_i]_{i=1}^n \\ [\rho_i]_{i=1}^n \end{bmatrix}}_{\mathcal{B}\text{,due to load}} + \underbrace{\begin{bmatrix} 0 & 0 \\ I & 0 \\ 0 & I \end{bmatrix}}_{\mathcal{C}} \begin{bmatrix} \Delta P_m \\ \Delta E_F \end{bmatrix} \tag{22}$$

where the various matrices on the RHS are as follows:

$$L = \begin{cases} L_{ik} = C_{2i}F_{1,ik} + C_{4i}F_{3,ik} & i \neq k \\ L_{ii} = C_{2i}F_{1,ii} + C_{3i} + C_{4i}F_{3,ii} \end{cases} \tag{23}$$

$$P = \begin{cases} P_{ik} = C_{2i}F_{2,ik} + C_{4i}F_{4,ik} & i \neq k \\ P_{ii} = C_{2i}F_{2,ii} + C_{1i} + C_{4i}F_{2,ii} \end{cases} \tag{24}$$

$$K = \begin{cases} K_{ik} = b_iF_{1,ik} + e_iF_{3,ik} & i \neq k \\ K_{ii} = b_iF_{1,ii} - e_i + e_iF_{3,ii} \end{cases} \tag{25}$$

$$J = \begin{cases} J_{ik} = b_iF_{2,ik} + e_iF_{4,ik} & i \neq k \\ J_{ii} = b_iF_{2,ii} + a_i + e_iF_{4,ii} \end{cases} \tag{26}$$

$$\gamma_i = C_{2i}G_{1i} + C_{4i}G_{2i} \tag{27}$$
$$\rho_i = b_iG_{1i} + e_iG_{2i} \tag{28}$$
$$D = \text{diag}(D_i),\ M = \text{diag}(M_i),\ T = \text{diag}(\tau_i) \tag{29}$$

and $P_m := [P_{mi}]_{i=1}^n$, $E_F := [E_{Fi}]_{i=1}^n$. The notation $[x_i]_{i\in\mathcal{S}}$ represents a column vector whose elements are x_i with i ranging in $\mathcal{S}$. Assuming PMUs are installed at designated buses whose indices are given by a set $\mathcal{S}$, the output equation can be formed as

$$y = [\Delta V_i,\ \Delta\theta_i]_{i\in\mathcal{S}}. \tag{30}$$

Equations (22)-(30) serve as the primary model for wide-area control indicating how the designable control inputs ΔP_m and ΔE_F enter the system dynamics. In Section VIII, for example, two new control paradigms will be introduced, both of which are based on the system model (22).

III. PMU Data Analysis & Model Identification

As indicated in Section II, all methods for Synchrophasor-enabled detection and control designs will need the underlying model (22) of the power system as a reference. However, since the operating conditions, the network topology, the load parameters and the controller settings of the machines are always changing over time, (22) needs to be *identified* using PMU measurements on-the-fly (or periodically, say every 15-20 minutes) so that the most latest model is available to the operator. This latest model can then be used for designing a plausible controller for oscillation damping when a disturbance happens in the system. The foremost problem that one must solve in order to construct a reliable model for the global network is, therefore, as follows:

Problem 1: Given $y = [\Delta V_i,\ \Delta\theta_i]_{i\in\mathcal{S}}$ in (30), develop *output-only* estimation techniques to estimate the parameters of the structured model (22) using $y(t)$. □

Since the excitation dynamics are typically much faster than the swing dynamics , the most important parameters to be estimated in Problem 1 are the machine inertias in M, the line reactances in L, and the load parameters in $\mathcal{B}$, all of which affect the swing oscillation modes. The reason for stating the term *'output-only'* in the above problem follows from the fact that the actual disturbance occurring in the system (for example, line loss, generation loss, line faults or controller failure in any machine in a remote corner of the network) may not be completely known at the time of estimation. Therefore, it is extremely difficult, if not impossible, to model the incoming disturbance as a mathematical function entering (22). Since output-only parameter estimation is inherently difficult, in many cases the effective impact of the fault or disturbance is considered to be a short-lived jolt, and, therefore, the input is modeled as a unit impulse function to facilitate identification of (22).

Yet another barrier for solving Problem 1 is the enormous size of the model (22), especially if the estimation has to be executed in real-time. Practically speaking, Problem 1, therefore, may be more relevant for the purpose of offline model validation than for real-time control. To a large extent,

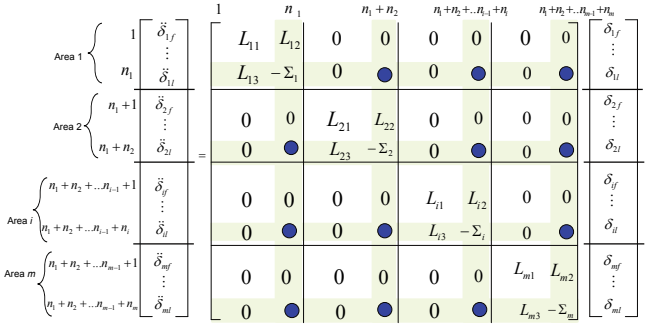

Fig. 2. Linearized Laplacian matrix denoting time-scale separation

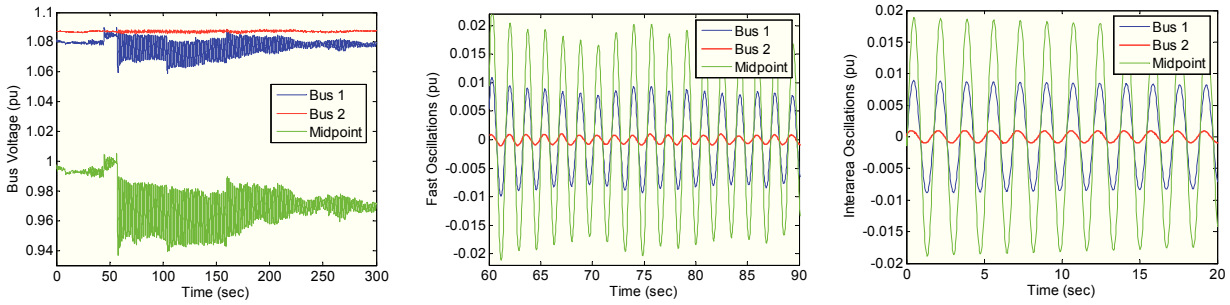

(a) PMU data from three buses (b) Band pass filtering (c) Slow oscillation mode

Fig. 3. Filtering and modal decomposition of PMU data from WECC

this problem is alleviated by the natural 'clustering' structure of any typical power system, arising from the differences in the tie-line reactances connecting one generator to another [23]. For example, if the network is divided into p coherent clusters or areas, separated by exactly one boundary node in each area, then the Laplacian matrix L in (22) can be written in the form shown in Figure 2. The blue dots indicate the *inter-area* coupling strengths between any pair of areas. The spectrum of L in that case will consist of three parts, namely: an eigenvalue at 0, and two non-intersecting sets $\mathcal{S}_1$ and $\mathcal{S}_2$, where $\mathcal{S}_1$ contains $(p-1)$ slow eigenvalues and $\mathcal{S}_2$ contains the remaining $(n-p)$ fast eigenvalues. The solutions of $\delta(t)$ and $\omega(t)$ in (22) will exhibit two-time-scale behavior, where the fast time-scale follows from the eigenvalues in $\mathcal{S}_1$, and the slow time-scale from those in $\mathcal{S}_2$.

Accordingly, the phase angle vector $\Delta\delta(t)$ can be projected into a partitioned vector of the form $\Delta\bar{\delta}(t) = [\Delta\delta_f \ \Delta\delta_s]$, where $\Delta\delta_f \in R^{n-p}$ represents the fast states and $\Delta\delta_s \in R^p$ represents the slow states. A constructive analysis of this behavior is also common in the literature [23]. For example, to obtain an analytical expression for the fast and slow oscillation dynamics, one may define the slow or aggregate variable for the k^{th} area as

$$\Delta\delta_k^s \triangleq \frac{\sum_{i=1}^{n_k} M_i^k \Delta\delta_i^k}{\sum_{i=1}^{n_k} M_i^k}, \quad k = 1, 2, ...p \tag{31}$$

where $\Delta\delta_i^k$ and M_i^k are, respectively, the i^{th} machine angle and inertia in the k^{th} area, n_k is the total number of machines in the k^{th} area, and p is the total number of areas. Similarly, the fast variable $\Delta\delta_k^f$ for the k^{th} area can be defined as:

$$\Delta\delta_k^f \triangleq \left[\Delta\delta_i^k - \Delta\delta_1^k\right]_{i=1}^{n_k} \qquad k = 1, 2, ...p. \tag{32}$$

Denoting $\Delta\delta_s = [\Delta\delta_k^s]_{k=1}^p$ and $\Delta\delta_f = [\Delta\delta_k^f]_{k=1}^p$, an equivalent representation of the swing dynamics in (22) can then be written as (ignoring the excitation system dynamics)

$$\Delta\ddot{\delta}_s = \mathcal{A}_{11}\Delta\delta_s + \mathcal{A}_{12}\Delta\delta_f + \mathcal{B}_1\Delta P_m \tag{33}$$

$$\epsilon\Delta\ddot{\delta}_f = \mathcal{A}_{21}\Delta\delta_s + \mathcal{A}_{22}\Delta\delta_f + \mathcal{B}_2\Delta P_m \tag{34}$$

where $\epsilon > 0$ is a small constant arising from the separation of the time-scales. Exact construction of the matrices $\mathcal{A}_{11}$, $\mathcal{A}_{12}$, $\mathcal{A}_{21}$, $\mathcal{A}_{22}$, $\mathcal{B}_1$ and $\mathcal{B}_2$ can be found in [23]. Substituting $\epsilon = 0$ in (34), and assuming A_{22} to be non-singular, one may write

$$\Delta\ddot{\delta}_s = \underbrace{(A_{11} - A_{12}A_{22}^{-1}A_{21})}_{\mathcal{A}_s}\Delta\delta_s + \underbrace{(\mathcal{B}_1 - \mathcal{A}_{22}^{-1}\mathcal{B}_2)}_{\mathcal{B}_s}\Delta P_m. \tag{35}$$

The p-dimensional reduced-order model (35) defines the slow time-scale dynamics of (22). A simpler version of Problem 1 can then be posed as follows.

Problem 2: Develop *output-only* estimation techniques to estimate the parameters of the structured model (35) using $y(t)$. □

In fact, Problem 2 may be more relevant in the context of wide-area control than Problem 1. The primary objective of wide-area oscillation damping, for example, is to damp the inter-area oscillation response of (22), which is equivalent to damping the slow time-scale behavior arising from (35). Power system operators, therefore, are often more interested in identifying (35) instead of (22) using $y(t)$. Equation (11) relates $y(t)$ to the linearized phase angle vector $\Delta\delta(t)$. The expression of $y_s(t)$ can, therefore, be obtained by substituting $\Delta\delta = \Delta\delta_s$ in (11). Due to the time-scale separation defined by (33)-(34) $y(t)$ can also be written as

$$y(t) = y_0 + y_s(t) + y_f(t) \tag{36}$$

where y_0 is the constant corresponding to the zero eigenvalue, $y_s(t)$ contains the contribution of the modes in $\mathcal{S}_1$ and $y_f(t)$ contains the contribution of the modes in $\mathcal{S}_2$, We next review some filtering and signal separation methods for estimating $y_s(t)$ from $y(t)$, and show an example on how $y_s(t)$ can be used to construct (35), as stated in Problem 2. We would like to note, however, that for both Problems 1 and 2 there is a fundamental question of identifiability, i. e., does $y(t)$ contain enough information to determine the unknown parameters uniquely? This parameter identifiability needs to be investigated for a deeper understanding of these two problems.

A. Filtering and Signal Separation

Before the voltage, phase angle, and frequency data can be used for identifying the dynamic model in (35), the measurements must be properly filtered and massaged with the objective of extracting the correct set of frequency components that are relevant to this model.

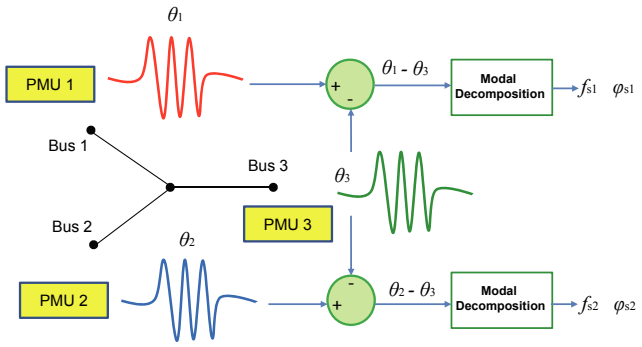

Fig. 4. Modal decomposition of multiple PMU data streams

Problem 2.1: Given $y(t)$ from (30), calculate $y_s(t)$. □

There can be both deterministic and stochastic versions of Problem 2.1. For example, if the PMU measurements in (30) are corrupted by noise, one would need to develop appropriate filtering techniques so that the accuracy of projecting $y(t)$ to $y_s(t)$ is maximum. Figure 3(a) shows the raw voltage oscillation measurements from three buses in the WECC system. Typically such measurements have both high frequency measurement noise and undesired low frequency oscillations arising from governor effects. If the goal is to construct the equivalent model (35) capturing the interarea oscillations that typically range between 0.1 to 1 Hz, then neither of these components are necessary for the estimation. A simple band pass filter, therefore, may be used to filter the raw data and retain its components only within the desired frequency range. Figure 3(b) shows the result of band pass filtering on the three bus voltage data shown in Figure 3(a). However, the outputs of the filter may still retain several modes that do not qualify as slow modes. A second round of filtering is, therefore, done by using subspace identification algorithms such as Eigenvalue Realization Algorithm (ERA). The computational scheme for applying ERA on multiple PMU data is shown in Figure 4, and can de described as follows. Consider a discrete-time LTI system

$$x(k+1) = A_d x(k) + Bu(k), \quad y(k) = Cx(k), \tag{37}$$

where $x(k) \in \mathbb{R}^n$ (n is known quantity), $k = 0, .., N$. The impulse response of the system will be given as

$$y(k) = CA_d^{k-1}B. \tag{38}$$

Given measurement $y(k)$, we next construct two $M \times p$ Hankel matrices H_0 and H_1 as:

$$H_0 = \left[\begin{array}{c|c|c|c} \mathbf{y}_0^0 & \mathbf{y}_1^0 & \cdots & \mathbf{y}_p^0 \end{array} \right], \tag{39a}$$
$$H_1 = \left[\begin{array}{c|c|c|c} \mathbf{y}_0^1 & \mathbf{y}_1^1 & \cdots & \mathbf{y}_p^1 \end{array} \right], \tag{39b}$$

where,

$$\mathbf{y}_i^0 = \left[y(i),\ y(i+1), \ldots,\ y(i+M-1)\right]^T, \tag{40a}$$
$$\mathbf{y}_i^1 = \left[y(i+1),\ y(i+2), \ldots,\ y(i+M)\right]^T. \tag{40b}$$

It can be easily shown that $H_0 = \mathcal{O}\mathcal{C}$ and $H_1 = \mathcal{O}A_d\mathcal{C}$, where $\mathcal{O}$ and $\mathcal{C}$ are observability and controllability matrices for (37), respectively. We next consider the truncated SVD of H_0 as:

$$\hat{H}_0 = \hat{R}\hat{\Sigma}\hat{S}^T. \tag{41}$$

Defining $E_p^T = [I_p\ 0_p\ \cdots\ 0_p]$ and $E_q^T = [I_q\ 0_q\ \cdots\ 0_q]$, where p and q are the number of inputs and outputs, respectively, estimates for triplet of $(\hat{A}, \hat{B}, \hat{C})$ can be easily calculated as follows:

$$\hat{A} = \hat{\Sigma}^{-1/2}\hat{R}^T H_1 \hat{S}\hat{\Sigma}^{-1/2}, \tag{42a}$$
$$\hat{B} = \hat{\Sigma}^{1/2}\hat{S}^T E_p, \quad \hat{C} = E_q^T \hat{R}\hat{\Sigma}^{1/2}. \tag{42b}$$

From $(\hat{A}, \hat{B}, \hat{C})$, one can write:

$$y(t) = \underbrace{\alpha_0}_{\text{DC value}} \underbrace{+\alpha_1 e^{\pm j\Omega_1 t} + \cdots + \alpha_{p-1}e^{\pm j\Omega_{p-1}t}}_{y_s(t),\ \text{slow oscillations}} + \underbrace{\alpha_p e^{\pm j\Omega_p t} + \cdots + \alpha_{n-1}e^{\pm j\Omega_{n-1}t}}_{y_f(t),\ \text{fast oscillations}}, \tag{43}$$

where, by assumption, there are $p-1$ slow modes (or, equivalently p areas). The constants α's and Ω's are known from estimation. By designating an upper bound on Ω_{p-1}, say 1 Hz, one can, therefore, easily extract $y^s(t)$ from $y(t)$ using (43).

B. Choice of Measurements

A pertinent question to answer before $y_s(t)$ can be employed for identifying a dynamic equivalent model is on how to choose the most optimal PMU locations for selecting the output vector $y(t)$, or to develop methods by which multiple measurements available from each area can be combined to construct $y(t)$. The accuracy of estimating $y_s(t)$ from $y(t)$ will indeed depend on several factors such as measurement noise, system structure, network topology, etc. [24]. Hence, any identification algorithm used for this projection may be associated with a corresponding metric of accuracy $\mathcal{I}$. To solve problem 2 one would need to select $y(t)$ from the available set of PMU data such that this metric is maximum. This is formally stated as follows.

Problem 2.2: Let m be the total number of installed PMUs. Consider that only $\tilde{m} \leq m$ of these PMUs are used for constructing $y_s(t)$ from $y(t)$. Let $\mathcal{I}(\mathcal{S})$ be the corresponding metric of accuracy for this projection, where $\mathcal{S}$ is the set of $\tilde{m}$ selected PMUs. Develop algorithms for selecting S to maximize $\mathcal{I}(\mathcal{S})$. □

If the machine inertias for any area are of the same order of magnitude, and the time-scale separation between the intra-area and inter-area dynamics as in (33)-(34) is well-defined, then all machines in that area will have almost similar slow oscillatory component of $\delta(t)$ and $\omega(t)$, respectively. Hence, phase angle and frequency measurements from any machine may be used as $y(t)$. If the values of M's in any given area are not available, one may consider the slow dynamics of the PMU data available from the boundary node(s) of that area as its equivalent slow dynamics. The choice follows from the fact that boundary nodes are connected to long inter-area transmission lines and, therefore, the slow modes have higher *participation factor* at these nodes [25].

C. Example

Consider a 5-cluster representation of the US west coast 500 KV grid as shown in Figure 5. The circles represent equivalent machines corresponding to the five major geographical regions on the coast, while the terminal buses denote their common points of interconnection. Without any loss of generality, we assume that every area is connected to every other area through an equivalent line with an equivalent impedance. Due to the presence of the PV buses, the state-space model for this system will be differential-algebraic, which can be converted to a completely differential model in the form of (22) using Kron reduction. However, as the objective of this reduced-order model is to capture only the inter-area oscillation modes it does not contain the effect of loads and excitation systems of every machine, and is approximated by a set of n interconnected swing equations only. The equivalent small-signal model can be derived as

$$\begin{bmatrix} \Delta\dot{\delta} \\ \Delta\dot{\omega} \end{bmatrix} = \begin{bmatrix} 0_{5\times5} & \omega_s I_{5\times5} \\ \text{diag}(\frac{-L}{M_i}) & -\text{diag}(\frac{2D_i}{M_i}) \end{bmatrix} \begin{bmatrix} \Delta\delta \\ \Delta\omega \end{bmatrix} + \begin{bmatrix} 0_{5\times5} \\ \text{diag}(\frac{1}{M_i}) \end{bmatrix} \Delta P_m \quad (44)$$

where

$$\begin{aligned} L_{ii} &= \frac{E_i}{x_i}\sin(\delta_i-\theta_i)F_{ii} - \frac{E_iV_i}{x_i}\cos(\delta_i-\theta_i)G_{ii} \\ &\quad + \frac{E_iV_i}{x_i}\cos(\delta_i-\theta_i) \\ L_{ik} &= \frac{E_i}{x_i}\sin(\delta_i-\theta_i)F_{ik} - \frac{E_iV_i}{x_i}\cos(\delta_i-\theta_i)G_{ik}, \end{aligned}$$

and the matrices F and G are given as

$$\begin{bmatrix} F \\ G \end{bmatrix} = \begin{bmatrix} \text{diag}(\cos(\theta_i)) & \text{diag}(\sin(\theta_i)) \\ \text{diag}(\frac{\sin(\theta_i)}{2V_R}) & \text{diag}(\frac{\cos^2(\theta_i)}{V_R}) \end{bmatrix} * \begin{bmatrix} -Y_R\text{diag}(E_I) - Y_I\text{diag}(E_R) \\ -Y_R\text{diag}(E_R) - Y_I\text{diag}(E_I) \end{bmatrix}. \quad (45)$$

Due to limitation in space, we refer the reader to [18] for the expressions for Y_R, Y_I, V_R, E_R and E_1. Considering that PMU measurements of voltage, phase angle and frequency are available from the terminal buses, the output equation can be written as

$$y(t) = \begin{bmatrix} \Delta V(t) \\ \Delta\theta(t) \\ \Delta f(t) \end{bmatrix} = \begin{bmatrix} F & 0 \\ G & 0 \\ 0 & \omega_s G \end{bmatrix} \begin{bmatrix} \Delta\delta(t) \\ \Delta\omega(t) \end{bmatrix}. \quad (46)$$

The components of the output vector $y(t)$ are passed through the ERA algorithm to extract the slow mode component $y_s(t)$ as in (43). The unknown parameters in (44) include the aggregate inertias of each equivalent machine, the internal impedance of each area connecting the machine internal node to its corresponding terminal bus, and the impedances of each transmission line. These parameters can be estimated from $y_s(t)$ using standard least squares techniques, assuming the input to be a unit impulse.

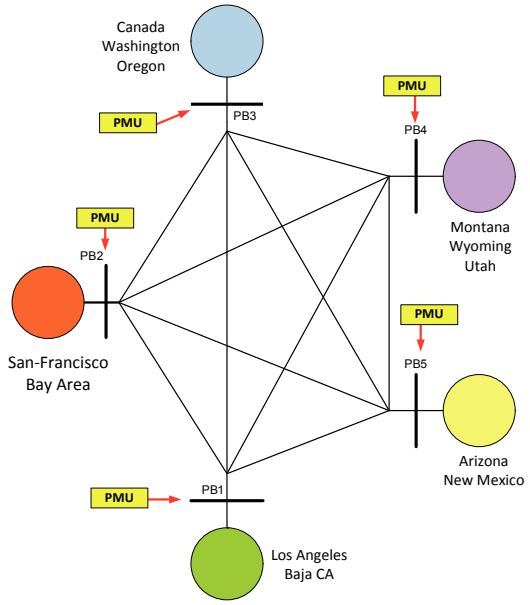

Fig. 5. 5 cluster representation of the US west coast grid

IV. Wide-area Power Oscillation Damping

Wide-area oscillation damping requires the design of either a centralized controller, for example using FACTS controllers such as Thyristor Controlled Series Compensator (TCSC) or Static VAr Compensator (SVC), or a set of distributed controllers such as wide-area Power System Stabilizers (PSS), that can provide a desired amount of closed-loop damping to the *slow* oscillation components in the phase angle oscillations, or equivalently, in the power flowing from one area to another. Damping local oscillations is relatively easy by using standard frequency feedback-based PSS designs, and, therefore, is not much of a concern for a wide-area problem. The basic set-up for wide-area damping control is as follows. Consider the power system network model (22), and define the control input as the excitation voltage E. Choose m number of generators in this network as candidates for implementing wide-area control through their respective exciters, the choice following from baseline analysis of which generators have highest participation factors on the inter-area modes of (22). Stack the measurements available for feedback to the j^{th} controller in the vector $y_j(t)$. Let $Y(t,\tau) = [y_j(t-\tau_j)]_{j=1}^m$, where τ_j is the signal transmission delay for communicating y_j to its corresponding controller, and τ is the vector of all such delays. The control problem can then be stated as follows.

Problem 3: Define a performance metric $\mathcal{J}$ to quantify the closed-loop damping of the slow eigenvalues of $\mathcal{A}$ in (22). Let $\mathcal{P}$ denote the set of models in (22)-(30) resulting from parameter variations in the system. Design an output-feedback dynamic controller $F(Y(t,\tau))$ that solves:

$$\min_F \max_{\mathcal{P}} \mathcal{J}. \quad (47)$$

□

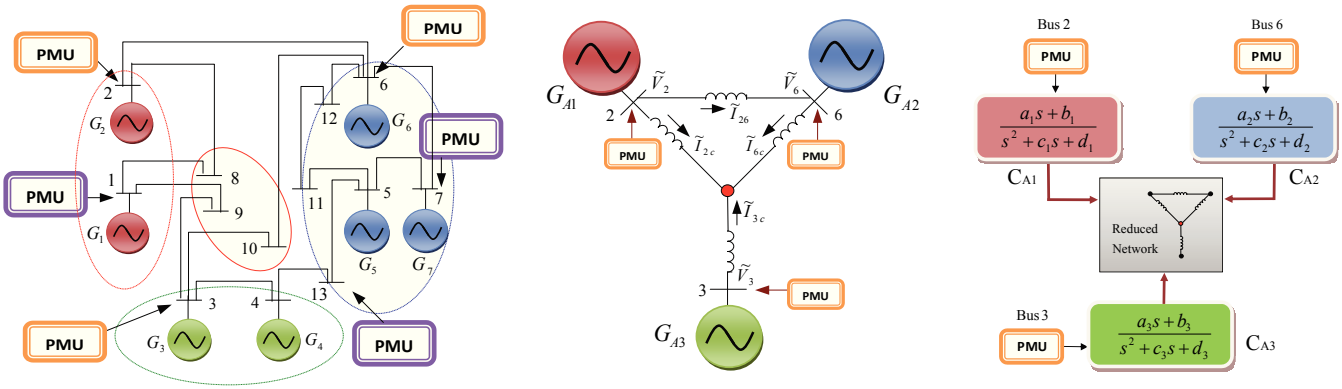

Fig. 6. Network of 7 generator nodes divided into 3 coherent areas

For example, $\mathcal{J}$ may be considered as the frequency weighted norm of the transfer matrix from disturbance inputs to an output vector containing the phase angle differences between the most critical buses in the system. A *control inversion* approach for designing $F(y(t))$ in (47) has recently been proposed in [26] loosely based on this idea. The approach consists of three main steps, namely: Identifying the dynamic equivalent model of the clustered power system model using available PMU measurements (Problem 2), designing hypothetical PSS controllers for the aggregated machine models in order to damp the inter-machine oscillations of power flow, and finally, inverting this control action by designing selected excitation controllers in the actual system so that (47) is satisfied. The performance metric $\mathcal{J}$ was chosen as the $\mathcal{L}_2$-norm of the difference between every pair of 'inter-area' phase angle in the full-order system and the corresponding inter-machine phase angle of the reduced-order system. The problem was posed as the design of an output-feedback controller $F(Y(t)$ that guarantees

$$\int_{t^*}^{t} ||x_{ij}(u(t)) - \bar{x}_{ij}(t)||_2^2 dt \leq \epsilon \tag{48}$$

for time $t \geq t^* \geq 0$, $u(t) = \text{col}(u_j(t))$, x_{ij} is the closed-loop inter-area state response (phase or/and frequency) between i^{th} and j^{th} areas, $\bar{x}_{ij}$ is the desired inter-area response of phase or/and frequency following from the reduced-order model, and $\epsilon > 0$ is a chosen tolerance for matching the two responses. For example, consider a 3-area power system shown in Figure 6, where Area 1 and 3 consist of two coherent machines each while Area 2 consists of three coherent machines, and, therefore, reduced to a three-machine equivalent interconnected through an equivalent graph. One may design a set of *hypothetical* excitation controllers or PSS for each of the three equivalent machines G_{A1}, G_{A2} and G_{A3}, using classical linear state-feedback designs. None of these controllers, however, can be implemented in practice as G_{A1}, G_{A2} and G_{A3} do not exist physically. Therefore, keeping the aggregate design as a reference, one next needs to design individual excitation controllers for each generator $G_1, G_2, ..., G_7$ in the 13-bus system of Figure 6, and tune them optimally until the *interarea* or slow oscillatory responses for the 13-bus system coincide with the closed-loop state responses of the 3-area system. Appropriate tuning can be achieved via various optimization methods. For example, one possibility can be to distribute the feedback gains of the aggregate controllers via continuous functions (for nonlinear control design) or averaging coefficients (for linear control design), and then to achieve interarea performance matching through optimal design of the controller parameters. Broadly speaking, the fundamental rationale behind this concept is that the feedback gains quantifying the closed-loop dynamics of a power system are substantially reflected in its electromechanical modes, and by extracting the frequencies and mode shapes of these modes from PMU measurements one can optimize these gains to achieve a desired interarea response.

V. Wide-Area Voltage Control

Wide-area voltage stability is a significant concern for power systems operating with remote generation and limited reactive power support along congested power transfer paths. Traditional methods of investigating voltage stability span two extremes. At one end of the spectrum, detailed models consisting of thousands of buses are used to calculate some voltage stability margins for many $N-1$ contingency cases [28]. At the other end of the spectrum, much simpler models of radial lines connected to a load center, also referred to as the voltage instability predictor (VIP) model, has been proposed [29]. This simple model is shown in Figure 7a. The realm of possible approaches for real-time voltage stability analysis changes substantially with the availability of PMUs, with new possibilities from both small-scale and large-scale PMU deployment. The VIP model can be made much more accurate by using PMU-based model reduction techniques, some of which have been discussed in the foregoing section. An example of such VIP model is shown in Figure 7. A pertinent problem to be solved, therefore, is:

Problem 4: Consider the VIP model shown for the q^{th} generator bus in a n-machine power system model given by (22). Using the PMU measurements from (30), estimate the equivalent generator parameters E'_q and Z^G_{Thev}, the equivalent load impedance Z_{agg}, and the equivalent controller parameters K_A and T. □

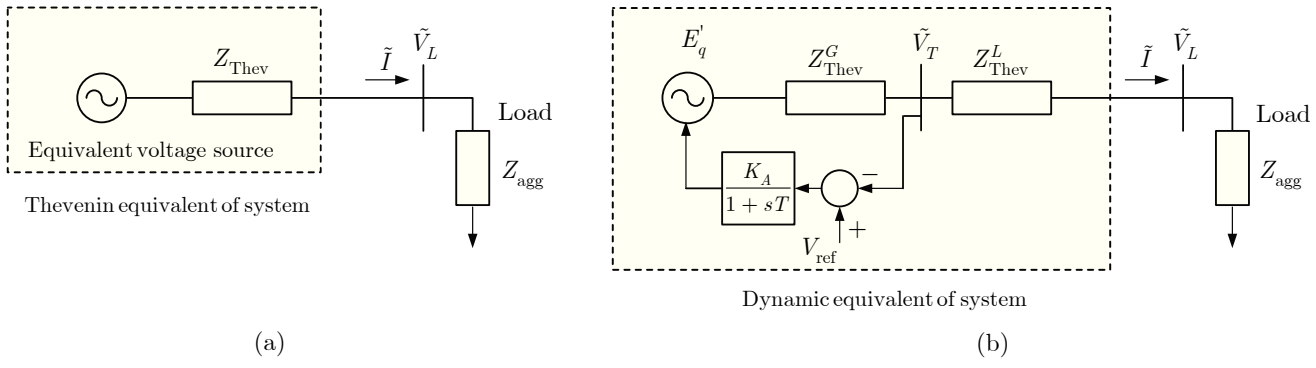

Fig. 7. Voltage stability models: (a) VIP model, and (b) dynamic VIP model

From a controls perspective, however, the primary application of Synchrophasors for mitigating voltage oscillations across wide areas lies in the control of voltage regulating devices such as Static VAr Compensators (SVC). Mathematically the problem can be described as follows. Consider a n-machine power system model defined over a network graph $\mathcal{G}$ with a graph Laplacian matrix L as in (22). Consider a bus j in this network, and assume the instantaneous voltage phasor at this bus at any time t to be $\tilde{V}_j(t) = V_j(t)\angle\theta_j(t)$. Consider that a voltage controller in the form of a Static VAr Compensator (SVC) or any other shunt FACTS device is installed at this bus to regulate V_j to a constant setpoint V_j^*. The dynamics of this controller is given as

$$\tau \dot{B}_j(t) = -B_j(t) + u_j(t) \tag{49}$$

where $B_j = \frac{1}{x_j}$ with x_j being the capacitive reactance which shorts Bus j to the ground voltage, as shown in Figure 8, and $u_j(t)$ is a designable input. Traditionally, a proportional controller of the form $u = k_j(V_j^* - V_j)$ is applied with $k_j > 0$ being the controller gain. Consider any other Bus i in the network with voltage phasor $\tilde{V}_i(t) = V_i(t)\angle\theta_i(t)$. Let the equilibrium values for $V_i(t)$ and $\theta_i(t)$ be V_0 and θ_0, respectively. Next, consider the following problem.

Problem 5: Evaluate the sensitivity of the voltage deviation $\Delta V_i(t) = V_i(t) - V_0(t)$, and angle deviation $\Delta\theta_i(t) = \theta_i(t) - \theta_0(t)$ with respect to the control gain k_j for any given i. Develop tools to analyze how these sensitivities depend on L. □

An analytical expression for such a sensitivity function was derived in [27] for a two-area radial system with intermediate voltage control. We next review those results to further motivate Problem 5. Consider a two-area power system, represented by two dynamic equivalent generators connected by an equivalent transmission line with an intermediate SVC controller, as shown in Figure 8. x_1 and x_2 denote the equivalent internal reactances of Area 1 and 2, respectively, while x_{e1} and x_{e2} are the reactances of the transmission line connecting the terminal buses of the areas to the SVC bus. For a general asymmetrical network we may define $\sigma_1 = x_1 + x_{e1}$ and $\sigma_2 = x_2 + x_{e2}$, and refer to the equivalent angular difference between the generators as simply δ. To show how k impacts the voltage magnitudes of other buses located at different points on the transfer path, consider the voltage phasor at any point between Bus 3 and Generator 2, at an 'electrical distance' or reactance of jx from Generator 2. The expression for this phasor can be derived as

$$\begin{aligned}\tilde{V} &= \left[E_2(1 - a_2 + a_2\frac{\sigma_1}{\chi}) + a_2(\frac{\sigma_2}{\chi})\, E_1\cos(\delta)\right] \\ &\quad + j\left[a_2(\frac{\sigma_2}{\chi})\, E_1\sin(\delta)\right]\end{aligned} \tag{50}$$

where, $a_2 = x/\sigma_2 \in [0,1]$ is the normalized distance, and $\chi(\delta) \triangleq \sigma_1 + \sigma_2 - B(\delta)\sigma_1\sigma_2$. We point the reader to [27] for more details of this derivation.

Following a small signal perturbation, the change in voltage magnitude at this point will be given by

$$\Delta V(t) = J(a_2, \delta_0)\Delta\delta(t) \tag{51}$$

where the Jacobian function is defined as

$$J(a_2, \delta_0) = \left.\frac{\partial|\tilde{V}|}{\partial\delta}\right|_{\delta=\delta_0} = \frac{1}{V_{ss}}\Upsilon_r(a_2, \chi, \chi', \delta_0). \tag{52}$$

Here, V_{ss} is the pre-disturbance equilibrium voltage at this location, and the expression for $\Upsilon_r(\cdot)$ can be found in [27], with all powers of $\chi(\delta)$ and $\chi'(\delta)$ computed at $\delta = \delta_0$. Given an equilibrium angle δ_0 the structure of $\chi(\delta_0)$ and $\chi'(\delta_0)$ in terms of E_1, E_2, σ_1, σ_2, k and V_r are known. Similarly, for the left half of the network (between Bus 3 and Generator 1), it can be shown that the change in voltage at a distance x from Bus 3 due to a change in δ is given as

$$J(a_1, \delta_0) = \left.\frac{\partial|\tilde{V}|}{\partial\delta}\right|_{\delta=\delta_0} = \frac{1}{V_{ss}}\Upsilon_l(a_1, \chi, \chi', \delta_0) \tag{53}$$

where $a_1 = x/\sigma_1 \in [0,1]$, and the expression for $\Upsilon_l(\cdot)$ can be found in [27], with all powers of $\chi(\delta)$ and $\chi'(\delta)$ computed at $\delta = \delta_0$. Figure 9 shows the variation of the normalized voltage at different points of the network from one end to the other, as given by the functions $\Upsilon_l(a_1)$ and $\Upsilon_r(a_2)$, for different SVC gains. To generate these plots we assumed $E_1 = E_2 = 1$ pu, $\delta_0 = 40^\circ$ and $V_r = 0.95$ pu. It can be seen that as the SVC gain increases the normalized voltage

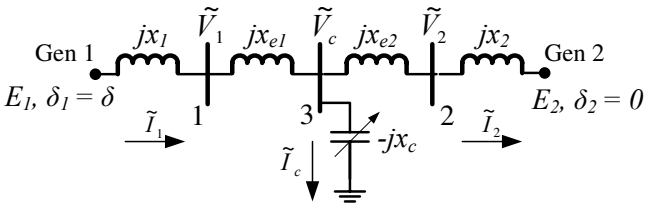

Fig. 8. Two-machine system with SVC

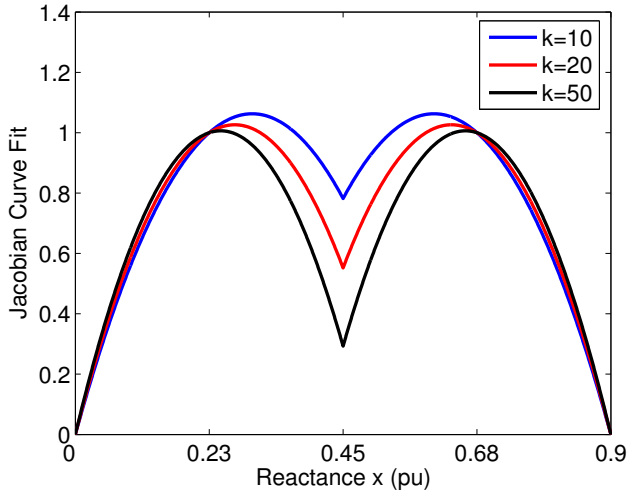

Fig. 9. Normalized voltage variation for two-area system with SVC

at Bus 3 approaches zero due to smaller voltage deviation from the setpoint caused by tighter voltage control.

An important observation made from Figure 9 is that for this two area system as the control gain of the SVC is increased for better voltage regulation, the voltage deviations at the other points on the tie-line increase from their pre-disturbance value. In other words, the voltage fluctuations at these spatial locations become more dominant due to the control action taken by the SVC. This naturally raises the question of how such local voltage control at one specific bus may impact other neighboring buses not just for a two-area system but for larger systems with multiple controllers and more arbitrary topologies. An example of such multi-area systems is shown in Figure 10, where four equivalent machines are connected by a meshed grid with eight SVCs located either on the border or at any intermediate grid point. Two pertinent problems, one on estimation and another on control, can then be stated as follows.

Problem 6: Consider the power system model (22) with m voltage regulators of the form (49) installed at m selected buses. Let the control gains of these regulators be $\mathcal{K} = (k_1, k_2, .., k_m)$. Derive how $|\tilde{V}_j(t)|$ at any bus j depends on $\mathcal{K}$.

Problem 7: Consider m SVCs installed at selected buses in the power system. Each SVC is defined by a model of the form (49) with corresponding control input u_i for the i^{th} SVC. Denote $u = [u]_{i=1}^m$. Let the measured output be $y(t)$ as in (30). Define a performance metric $\mathcal{J}$ that reflects the deviation of the voltage at any bus j from its setpoint for $j = 1, 2, .., n$. Design an output-feedback dynamic controller $u(t) = F(y(t))$ that minimizes $\mathcal{J}$.

However, as illustrated by the two-machine example, there are likely to be fundamental constraints that will impose lower bounds on the best achievable closed-loop control performance for Problem 7. Quantification of such lower bounds will be an interesting direction that could yield fundamental new insights into the network-level voltage control problem.

VI. Wide-Area Disturbance Localization

A critical aspect of wide-area control, as substantiated by the power oscillation damping and voltage control problems discussed above, is to capture the 'spatial' impacts of various complex physical phenomenon arising in the grid, and controlling their undesired effects coupling various parts of this spatial domain. From a modeling point of view this demands a fundamental understanding of how major disturbances typically *attack* a large power grid, how the resulting *dynamic* effects disseminate or 'spread' through the network in the form of oscillatory electrical modes, and the ways in which the network components and the network *structure* help or impede the propagation of these disturbance modes. For example, Consider the n-machine power system model (22) rewritten in the following form:

$$\begin{bmatrix} \Delta\dot{\delta} \\ M\Delta\dot{\omega} \\ T\Delta\dot{E} \end{bmatrix} = \begin{bmatrix} 0 & I & 0 \\ -L & -D & -P \\ K & 0 & J \end{bmatrix} \begin{bmatrix} \Delta\delta \\ \Delta\omega \\ \Delta E \end{bmatrix} + \underbrace{\begin{bmatrix} 0 \\ [\gamma_i]_{i=1}^n \\ [\rho_i]_{i=1}^n \end{bmatrix}}_{\text{due to load}} + \begin{bmatrix} 0 & 0 \\ \mathcal{E}_1 & 0 \\ 0 & \mathcal{E}_2 \end{bmatrix} \begin{bmatrix} f_1(t) \\ f_2(t) \end{bmatrix}. \quad (54)$$

Assume that the system already operates in closed-loop, due to which the effect of the control inputs ΔP_m and ΔE are not considered separately in (54). Two additional input vectors $f_1(t) \in R^n$ and $f_2(t) \in R^n$ are, however, added to model the intrusion of extraneous time-varying *influence* signals. The extraneous input $f_2(t)$ model the effects of internal failures of controllers and actuators, which are most likely to enter the system equations through the excitation system dynamics. The input $f_1(t)$, on the other hand, can be a malicious attack vector that may be purposely injected to the swing dynamics via manipulation of power flow or by corrupted control feedback. $\mathcal{E}_1$ and $\mathcal{E}_2$ are sparse $n \times n$ indicator matrices with binary entries, where $\mathcal{E}_1(i,j) = 1$ means that the i^{th} generator is influenced by the malicious 'attack' function $f_{1j}(t)$, while $\mathcal{E}_2(i,j) = 1$ means that the excitation system of the i^{th} generator is biased by the controller failure function $f_{2j}(t)$. The localization problem can then be stated simply as:

Problem 8: Estimate the locations of the non-zero entries of $\mathcal{E}_1$ and $\mathcal{E}_2$ using the PMU measurements in (30), assuming nominal knowledge of the input functions $f_1(t)$ and $f_2(t)$.□

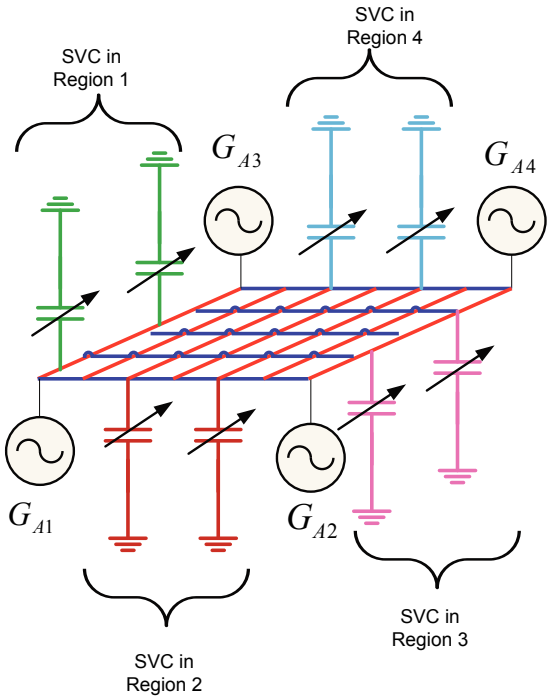

Fig. 10. Voltage interactions over a wide-area 2-d grid

An identification-based approach has been proposed recently in [32] where graph-theoretic and system-theoretic properties of the power network are combined to develop weak nodal domains spanning various coherent areas in the system. These nodal domains are related to the residues of the transfer function, which, in turn, can be identified using PMU data, and the signs of the residues are used for accurate localization of any disturbance occurring within an area.

VII. New Control Paradigms

In this section we present two design ideas for wide-area control using the model identification concepts described in Problems 1 and 2 above. Although the designs are primarily focused on the problem on power oscillation damping, they are equally applicable for voltage and frequency (AGC) control problems. Our first idea is based on a centralized scheme that selects an optimal controller from a set of multiple controllers depending on the fault condition. The second design is a distributed control design where state estimates are exchanged between area-level controllers over a secure communication network.

A. Multiple Controller Scheduling

Consider a p-area power system, and let G_i and G_j denote any of the boundary generators of the i^{th} and j^{th} areas. Assume that the two generators are connected by an equivalent radial tie-line. A Thyristor Controlled Series Compensator (TCSC) is installed across this long line to regulate the effective reactance, or equivalently the effective power flowing from one area to another. PMUs are installed at the boundary buses, and, hence, the phase angle and frequency measurements from G_i and G_j, or some reliable estimates of them, are available. We will use the TCSC as a controller for providing inter-area power oscillation damping using Synchrophasor feedback from these boundary buses. The total reactance between the internal nodes of G_p and G_q can be written as

$$\tilde{x}_{ij} = x'_{d,i} + x'_{d,j} + x_{ij} + \Delta x_{ij}(t) =: \bar{x}_{ij} + \Delta x_{ij}(t) \quad (55)$$

where $x'_{d,i} > 0$ denotes the direct-axis transient reactance of the i^{th} machine, $x_{ij} > 0$ is a fixed nominal tie-line reactance, and $\Delta x_{ij}(t)$ is a variable tie-line reactance that can be controlled via TCSC. $\bar{x}_{ij} > 0$ denotes the fixed part of the total reactance. The relative swing dynamics between these two generators, neglecting damping, coupled with first-order TCSC dynamics, can be written as [31]

$$\frac{2H_iH_j}{H_i+H_j}\dot{\omega}_{ij} = \bar{P}_m - l_{f,ij}(\delta) - \frac{E_iE_j\sin(\delta_{ij})}{\bar{x}_{ij}+\Delta x_{ij}(t)} \quad (56)$$

$$\dot{\delta}_{ij} = \omega_{ij}, \quad T_{ij}\Delta\dot{x}_{ij} = -\Delta x_{ij} + u_{ij}, \quad (57)$$

where, $\delta_{ij} = \delta_i - \delta_j$, $\bar{P}_m$ is the relative mechanical power input scaled by the inertias [18], and the scalar function $l_{f,ij}(\cdot)$ models the power flows internal to the i^{th} and j^{th} areas as well as those between these two areas and their neighboring areas. u_{ij} is a designable input for the TCSC located between Bus i and j. Linearizing the system about a chosen equilibrium, and denoting the state vector simply as x, the swing model of the p-area system can be represented as

$$\dot{x} = A(w)x, \quad \epsilon\dot{w} = f(w) + u \quad (58)$$

where $w \in \mathbb{R}$ is the designable admittance of the long tie-line, the scalar function $f(\cdot)$ models the TCSC dynamics, $\epsilon = T_{pq} > 0$ is a small constant, and u is the control input to the TCSC to be designed via Synchrophasor feedback. Let the measured outputs be stacked in the vector $Y(t)$, and let the set of transmission delays for communicating remotely located phasors to the TCSC site be τ. Given the controller structure (58), the wide-area control design problem is stated as follows:

Problem 9: Define a performance metric $\mathcal{J}$ for the system (58) to quantify the closed-loop damping of the slow eigenvalues of $A(w)$. Denoting $A(w)$ to be the set of all possible models resulting from parameter variation, design an output-feedback dynamic controller $F(Y(t,\tau), w^*)$ that solves:

$$\min_{F} \max_{\mathcal{A}(w)} \mathcal{J}. \quad (59)$$

where $w^* > 0$ is a constant that may be chosen from a prior set of weights according to the disturbance event defining the matrix $A(w)$. □

One approach to solve Problem 7 can be based on the following steps:

Step 1: Consider a set of *most probable* disturbance events in the system, such as loss of a typical set of lines or generators, or perhaps line-to-ground or line-to-line faults in the most probable locations. For each of these events, measure the angular difference $y(t) = (x_i(t) - x_j(t))$

between the boundary buses, pass this signal through the ERA algorithm, and extract its slow response. Considering N 'planned' events, let the set of the identified slow responses be denoted as

$$Y_s = \{y_{s1}(t),\, y_{s2}(t), ..., y_{sN}(t)\},\quad t \in [t_0 : \Delta T : t_f]. \quad (60)$$

Step 2: Design a digital FIR filter

$$G(z) = \sum_{i=1}^{M} a_i z^{-i} \quad (61)$$

such that, if $y(t) = (x_p(t) - x_q(t))$ for each event is passed through this filter, then the outputs match the corresponding entries of Y_s as much as possible. Mathematically, this can be posed as

$$\min_{a} \frac{1}{N} \sum_{i=1}^{N} ||G(z)[y_k](t) - y_{si}(t)||_2^2 \quad (62)$$

where, a is the set of filter coefficients a_i, and the subscript k denotes the k^{th} event.

Step 3: Consider the open loop plant dynamics in (58), i.e., $\dot{x} = A(w)x$ for each of the N planned events, and design a corresponding weight w_i, for $i = 1, 2, .., N$, such that the signal $\tilde{y}_i(t) \triangleq G(z)[y_i](t)$ has a desired damping. Repeat this design for all N events, and define the weight set $W = \{w_1,\, w_2, ..., w_N\}$.

Step 4: When an actual disturbance event happens, initially employ a phase angle feedback of

$$u = k\,(G(z)[(x_i(t-\tau_i) - x_j(t-\tau_j))](t). \quad (63)$$

where k is a feedback gain. In parallel, employ very fast estimation algorithms on the data available from all the PMUs in the system, to detect the type and location of the event, for example by using some of the input localization methods discussed in Section VI. Once the event type is estimated, the corresponding pre-designed weight w^* for that event can be selected from the set W, and the speed of the closed-loop damping control can be increased by re-actuating the control as

$$u = k(G(z)[(x_i(t-\tau_i) - x_j(t-\tau_j))](t) + w^*. \quad (64)$$

The *wide-area* aspect of the design (64) is clear from the fact that it involves transmission of the two remote PMU signals $x_i(t)$ and $x_j(t)$ to the controller site. The actual closed-loop response will, therefore, involve the impacts of all typical communication-related uncertainties such as delays, data dropouts, noise, and data corruption due to cyber-physical failures. The design can also be easily extended to a multi-area power system with multiple sets of TCSCs operating across a chosen set of tie-lines. The choice of the weights w^* for all the TCSCs in such cases, however, will be dependent on each other due to the inherent coupling between the interarea dynamics. One pertinent research challenge for this problem, therefore, will be to minimize the amount of time taken to detect the origin of the disturbance from all available PMU data, and to select the optimal set of w^*'s from the apriori designed gains.

B. Distributed Control

A more attractive choice for implementing a wide-area control scheme is to employ distributed controllers that stabilize the global system dynamics in face of various disturbances, and at the same time guarantee a desired closed-loop performance for both local and interarea oscillations in the voltage and phase angles at different critical buses. For example for the three-area system of Figure 6, one may choose two generators in Area 1, two in Area 2, and three in Area 3, and design individual PSS for these 7 generators in a distributed fashion to shape the closed-loop response of the fast and slow oscillations for the entire system. Mathematically, the problem can be posed as follows. Let the state-variable model for the i^{th} chosen generator with a tunable PSS, for $i = 1, ...p$, be given as

$$\dot{x}_i = f_i(x) + g_i(x)u_i \quad (65)$$

where u is the excitation control feedback for the PSS. Let $\mathcal{M}$ be the set of bus indices where a PMU is installed, and $\mathcal{M}^i$ be the subset of $\mathcal{M}$ that are available for output-feedback to the i^{th} PSS. The measurements in the set $\mathcal{M}^i$ are denoted as $y_{\mathcal{M}^i}(t)$. Let the set of boundary buses separating the areas be $\mathcal{E}_b$, and the communication graph between the different controllers be $\mathcal{G}$. The distributed control problem then reduces to the following problem.

Problem 10: Design the control function $\psi(\cdot)$ for

$$u_i(t) = \psi_i(y_{\mathcal{M}^i}(t), x_{j\in\mathcal{N}_i}(t-\tau_{ij}), t),\quad i = 1, .., p \quad (66)$$

where $\mathcal{N}_i$ is the neighbor set of i^{th} controller following from $\mathcal{G}$, and τ_{ij} is the communication delay in the channel connecting the i^{th} and j^{th} controllers, such that all closed-loop state responses are bounded over time, and the 'slow' oscillation components of the relative phase angle difference $x_{pq}(t) \triangleq (x_p(t) - x_q(t))$ between every pair of boundary nodes $(p, q) \in \mathcal{E}_b$ satisfy a desired response. □

In other words, the distributed controller (66) must solve

$$\min ||G(z)[x_{pq}](t) - x^d_{pq}(t)||_2,\ \ \forall (p, q) \in \mathcal{E}_b \quad (67)$$

where, $x(t)$ is bounded, $x^d_{pq}(t)$ is a desired power flow response, and $G(z)$ is an optimal FIR filter that mimics the filtering effect of subspace ID, as discussed in Section VIIA. It is evident that the distributed optimal control problem (66)-(67) opens up a wealth of research directions for control theorists. For example, thorough investigation is needed to test the applicability of various distributed optimization methods such as Lagrangian techniques to solve (67). The impacts of communication network uncertainties such as the statistical distributions associated with the delays τ_{ij}, and other design factors such as optimal partitioning of the measurement sets $\mathcal{M}^i$ into the various PSSs, on the solutions of (67) are yet other important topics that need attention from this research community.

VIII. Conclusions

This tutorial paper serves as a technical invitation to enter the challenging and attractive research field of wide-area

control of power systems. We presented an overview of the main research ideas related to this topic, and established a strong dependence of control on ideas of measurement-based model reduction. Evidently, there are several challenges that need to be surmounted in order to implement the proposed designs, three most important of which are:

• *Scalability* - As the number of PMUs scale up to the thousands in the next five years in the US, the proposed control schemes and their communication schemes must be able to handle the massive volumes of data,

• *Real-time processing* - since a sufficient number of data points (estimation bandwidth) would be required for these controllers, data handling issues such as proper file formatting, missing data points, incorrectly aligned data, file storage and database management will naturally arise,

• *Communication mechanisms* - Perhaps the most important challenge is to integrate the distributed control algorithms with state-of-art communication network architectures such as NASPInet using IEEE C37.118 or IEC 61850 protocols. A network architecture which implements IP networking technologies, including IP multicast, will need to be constructed for the transport of PMU data within a single network domain (that is, a single utility), or between network domains or multiple utilities. These domains can consist of service components such as phasor data concentrators (PDC), data historians and phasor gateways [33].

Solving these challenges need a strong knowledge of stochastic modeling, estimation theory, embedded control and optimization. It is, therefore, our hope that this topic will be viewed by budding and established control theorists as a challenging and attractive opportunity for their skills and talents. The compelling societal importance of energy systems would suffice as additional motivation to enter this endeavor.

REFERENCES

[1] A. G. Phadke, J. S. Thorp, and M. G. Adamiak, "New Measurement Techniques for Tracking Voltage Phasors, Local System Frequency, and Rate of Change of Frequency," *IEEE Transactions on Power Apparatus and Systems*, vol. 102, pp. 1025-1038, May 1983.

[2] North American Synchrophasor Initiative - *www.naspi.org*

[3] WISP - *http://www.wecc.biz/awareness/Pages/WISP.aspx*

[4] J. F. Hauer, D. J. Trudnowski, G. J. Rogers, W. A. Mittelstadt, W. H. Litzenberger, and J. M. Johnson, "Keeping an Eye on Power System Dynamics," *IEEE Computer Applications in Power*, pp. 50-54, 1997.

[5] M. Parashar and J. Mo, "Real Time Dynamics Monitoring System: Phasor Applications for the Control Room," 42^{nd} *Hawaii International Conference on System Sciences*, pp. 1-11, 2009.

[6] Y. Liu *et al.*, "A US-Wide Power Systems Frequency Monitoring Network," *Proceedings of the IEEE PES General Meeting*, Montreal, QC, Canada, June 2006.

[7] C. Ray and H. Huang, "Power Grid Dynamics: Enhancing Power System Operation through Prony Analysis," *U. S. Department of Energy Journal of Undergraduate Research*, vol. VII, pp. 87-90, 2007.

[8] N. Zhou, J. W Pierre, D. J Trudnowski, and R. T Guttromson, "Robust RLS methods for Online Estimation of Power System Electromechanical Modes," *IEEE Transactions on Power Systems,* vol. 22(3), 2007.

[9] J. Quintero, G. Liu, and M. Venkatasubramanian, "An Oscillation Monitoring System for Real-time Detection of Small-Signal Instability in Large Electric Power Systems," *IEEE Power Engineering Society General Meeting*, June 2007.

[10] A. R. Messina, V. Vittal, D. Ruiz-Vega, and G. Enriquez-Harper, "Interpretation and Visualization of Wide-area PMU measurements using Hilbert Analysis," *IEEE Transactions Power Systems*, vol. 21(4), pp. 1760-1771, 2006.

[11] R. Emami and A. Abur, "Reliable Placement of Synchronized Phasor Measurements on Network Branches," *IEEE PSCE*, Seattle, WA, March 15-19, 2009.

[12] G. K. Stefopoulos, R. H. Alaileh, G.. Cokkinides and A. P. Meliopoulos, "On Three-Phase State Estimation in the Presence of GPS-Synchronized Phasor Measurements," *Proceedings of* 39^{th} *North American Power Symposium* (NAPS), pp. 406-412, 2007.

[13] L. Vanfretti, J. H. Chow, S. Sarawgi, and B. Fardanesh, "A Phasor-Data-Based State Estimator Incorporating Phase Bias Correction," *IEEE Transactions on Power Systems,* vol. 26(1), pp. 111-119, 2010.

[14] C.W. Taylor, D.C. Erickson, K.E. Martin, R.W. Wilson, and V. Venkatasubramanian, "WACS Wide-Area Stability and Voltage Control System: R & D and Online Demonstration," *Proceedings of the IEEE*, vol. 93(5), pp 892-906, May 2005.

[15] I. Kamwa, R Grondin, and Y. Hebert, "Wide-Area Measurement Based Stabilizing Control of Large Power SystemsA Decentralized/Hierarchical Approach," *IEEE Transactions on Power Systems*, vol. 16(1), pp. 136-153, 2001.

[16] N. R. Chaudhuri, D. Chakraborty, and B. Chaudhuri, "Damping Control in Power Systems Under Constrained Communication Bandwidth: A Predictor Corrector Strategy," *IEEE Transactions on Control Systems Technology,* vol. 20(1), pp. 223-231, Jan 2012.

[17] N. R. Chaudhuri, A. Domahidi, B. Chaudhuri, R. Majumder, P. Korba, S. Ray, and K. Uhlen, "Power Oscillation Damping Control Using Wide-Area Signals: A Case Study on Nordic Equivalent System," *IEEE PES T&D Conference and Exposition*, 2010.

[18] P. M Anderson and A. A. Fouad, *Power System Control and Stability*, 2^{nd} Edition, Wiley Interscience, 2002.

[19] P. Varaiya, F. Wu, and R. Chen, "Direct Methods for Transient Stability Analysis of Power Systems: Recent Results," *Proceedings of IEEE*, vol. 73, no. 12, pp. 1703-1714, Dec. 1985.

[20] P. Kundur, *Power System Stability and Control*, McGraw-Hill, 1994.

[21] W. Dib, R. Ortega, A. Barabanov, F. Lamnabhi-Lagarrigue, "A Globally Convergent Controller for Transient Stability of Multi-Machine Power Systems Using Structure Preserving Models," *IEEE Conference on Decision and Control*, pp. 4431-4437, Cancun, Mexico, Dec. 2008.

[22] A. Chakrabortty and P. Khargonekar, "Introduction to Wide-Area Monitoring and Control," *Internal Report*, Available at: *http://people.engr.ncsu.edu/achakra2/wacs.pdf*.

[23] J. H. Chow, G. Peponides, P. V. Kokotovic, B. Avramovic, and J. R. Winkelman, *Time-Scale Modeling of Dynamic Networks with Applications to Power Systems*, Springer-Verlag, NY, 1982.

[24] L. Ljung, *System Identification: Theory for the User*, 2^{nd} Edition, Prentice Hall, NJ, 1999.

[25] B. Pal and B. Chaudhuri, *Robust Control in Power Systems,* Springer, 2005.

[26] A. Chakrabortty, "Wide-Area Damping Control of Power Systems Using Dynamic Clustering and TCSC-Based Redesigns," *IEEE Transactions on Smart Grid*, vol. 2(3), Nov. 2012.

[27] A. Chakrabortty, J. H. Chow and A. Salazar, "A Measurement-based Framework for Dynamic Equivalencing of Power Systems using Wide-Area Phasor Measurements," *IEEE Transactions on Smart Grid*, vol. 1(2), pp. 68-81, 2011.

[28] H.-D. Chiang, H. Li, J. Tong, and P. Causgrove, "On-line voltage stability monitoring of large power systems," *Proceedings of IEEE PES GM*, Detroit, MI, July 2011.

[29] D. E. Julian, R. P. Schulz, K. T. Vu, W. H. Quaintance, N. B. Bhatt, and D. Novosel, "Quantifying Proximity to Voltage Collapse using the Voltage Instability Predictor (VIP)," *Proc. IEEE PES Summer Power Meeting*, July 2000, vol. 2, pp. 931-936.

[30] S. Arabi, H. Hamadanizadeh, and B. Fardanesh, "CSC Performance Studies on the NY State Transmission System," *IEEE Transactions on Power Systems*, vol. 17(3), pp. 701-706, 2002.

[31] N. G. Hingorani and L. Gyugyi, *Understanding FACTS*, IEEE Press, NY, 2000.

[32] T. R. Nudell and A. Chakrabortty, "Measurement-Based Methods for Disturbance Localization in Large Power Grids," *proceedings of American Control Conference,* DC, 2013.

[33] R. Hasan, R. Bobba and H. Khurana, "Analyzing NASPInet Data Flows," *IEEE Power Systems Conference and Exposition* (PSCE '09), Seattle, WA, March 2009.